# Quantum Dot-based Electrochemical Biosensor for Stripping Voltammetric Detection of Telomerase at the Single-Cell Level

Chen-chen Li, Juan Hu, Mengfei Lu, Chun-yang Zhang

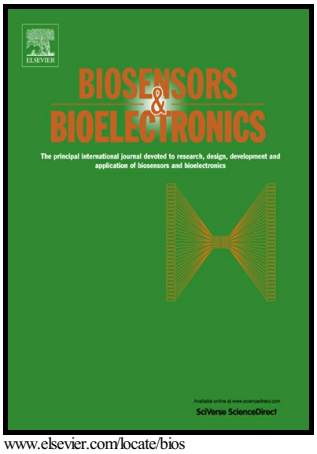


www.elsevier.com/locate/bios

PII: S0956-5663(18)30740-1
DOI: https://doi.org/10.1016/j.bios.2018.09.049
Reference: BIOS10789

To appear in: *Biosensors and Bioelectronic*

Received date: 23 July 2018
Revised date: 30 August 2018
Accepted date: 12 September 2018

Cite this article as: Chen-chen Li, Juan Hu, Mengfei Lu and Chun-yang Zhang, Quantum Dot-based Electrochemical Biosensor for Stripping Voltammetric Detection of Telomerase at the Single-Cell Level, *Biosensors and Bioelectronic,* https://doi.org/10.1016/j.bios.2018.09.049

# Quantum Dot-based Electrochemical Biosensor for Stripping Voltammetric Detection of Telomerase at the Single-Cell Level

Chen-chen Li[1], Juan Hu[1], Mengfei Lu[†], Chun-yang Zhang[*]

College of Chemistry, Chemical Engineering and Materials Science, Collaborative Innovation Center of Functionalized Probes for Chemical Imaging in Universities of Shandong, Key Laboratory of Molecular and Nano Probes, Ministry of Education, Shandong Provincial Key Laboratory of Clean Production of Fine Chemicals, Shandong Normal University, Jinan 250014, PR China.

[*]Corresponding author. Tel.: +86 0531-86186033; fax: +86 0531-82615258. cyzhang@sdnu.edu.cn.



**Abstract**

Human telomerase is responsible for the maintenance of chromosome end structures and is a valuable biomarker for malignant growth. However, the accurate measurement of telomerase activity at the single-cell level has remained a great challenge. Here we develop a simple quantum dot (QD)-based electrochemical biosensor for stripping voltammetric detection of telomerase activity at the single-cell level. We designed a thiol-modified capture DNA which may be immobilized on the gold electrode by the gold-sulfur bond. The presence of telomerase enables the addition of the telomere repeats of $(TTAGGG)_n$ to the 3' end of the primer, accompanied by the incorporation of abundant biotins in the extension product with the assistance of the biotin-tagged dATP. The subsequent hybridization of extension product with the capture DNA and the addition of streptavidin-coated QDs induce the assembly of large amounts of QDs onto the electrode via specific biotin-streptavidin binding. After the acidic dissolution of QDs, the released Cd (II) can be simply quantified by anodic stripping voltammetry (ASV). Due to the introduction of large amounts of QDs by telomerase-induced primer extension reaction and the synergistic signal amplification induced by the release of Cd (II) from the QDs, this biosensor can detect telomerase activity at the single-cell level without the involvement of any thermal cycling and extra enzymes for signal amplification. Moreover, this assay exhibits

[1] These authors contributed equally.

a large dynamic range over four orders of magnitude and it is very simple without the involvement of specific hairpin probe design and complicated labelling, holding great potential in point-of-need testing.

**Keywords: electrochemical sensing, quantum dot, telomerase, single-cell level**

## 1. Introduction

Human telomerase, a ribonucleoprotein complex, can synthesize single-stranded telomeric repeats $(TTAGGG)_n$ to keep the stability of telomere length by utilizing its internal RNA as a template and its reverse transcriptase protein as polymerase (Cohen et al. 2007; Collins and Mitchell 2002; Stone et al. 2007). Telomere can protect the ends of linear chromosomes from degradation and repair activities, and it is essential to the maintenance of chromosome stability. The telomerase deficiency-induced excessive telomere shortening may trigger a DNA damage response, and the dysfunctional telomeres may lead to cancer and ageing pathology (Blackburn 2001; Martinez and Blasco 2011). Moreover, telomerase is reactivated or up-regulated in most types of malignant cancer cells (Harley 2008; Shay and Wright 2011), and it may function as a diagnostic and prognostic marker as well as a potential target for cancer therapy (Arndt and MacKenzie 2016; Wang et al. 2017a). Thus, the rapid and sensitive detection of telomerase activity is important for better understanding its role in cancer cells, clinical diagnosis and anticancer drugs discovery.

The conventional telomeric repeat amplification protocol (TRAP) has become the gold standard for detecting telomerase activity in small number of cells and tissue extracts, but it involves polymerase chain reaction (PCR) with strict thermal cycling (Kim et al. 1994; Su et al. 2018). Although quite powerful, the gel electrophoresis-based assay suffers from the risk of carry-over contamination, susceptibility to polymerase inhibition by cell extract, laborious post-PCR processing, and the requirement of expensive equipment and reagents (De Cian et al. 2007; Xiao et al. 2010). Alternatively, some PCR-free approaches have been developed to overcome these issues, including exponential isothermal amplification of telomere repeat (Tian and Weizmann 2013), primer-generation rolling circle amplification (Ma et al. 2018), and T7-exonuclease-assisted target recycling amplification (Wang et al. 2012a). These isothermal amplification methods are much simpler than the PCR-based TRAP assay, but they usually involve the complicated template and probe design, the use of a special exonuclease, special DNA polymerases and nicking

endonucleases, inevitably increasing the experimental complexity and cost. To simplify the experimental procedure and improve the detection sensitivity, some nanomaterial-based amplification approaches have been introduced, including the use of liposomal signal amplification (Alizadeh-Ghodsi et al. 2016), functionalized upconversion nanoparticles (Wang et al. 2015a), Pt nanoparticle-mediated catalyzation of $H_2O_2$ decomposition (Wang et al. 2017b), DNAzyme and luminol-modified Au nanoparticles as the double-catalytic amplification labels (Zhang et al. 2014). But most of them are used for imaging applications (Qian et al. 2013; Sharon et al. 2014; Wang et al. 2015b), and new strategies for simple and accurate measurement of telomerase activity are still highly desirable.

The nanoparticles such as Au nanoparticles and $Fe_3O_4$ magnetic nanoparticles consist of thousands of atoms which can be oxidized or reduced electrochemically and can act as the electroactive labels for signal amplification in electrochemical measurement (Cui et al. 2018; Wang et al. 2012b; Zhang et al. 2017). For example, the chemical oxidation of nanolabels (e.g., ZnS, CdS, and PbS quantum dots) may result in the release of abundant metal cations which can be simply measured by anodic stripping voltammetry (ASV) (Gao et al. 2016; Wang et al. 2003). The noble metal nanoparticles (e.g., AuNPs and AgNPs) (Chumbimuni-Torres et al. 2006; Zhu et al. 2013) and quantum dots (QDs) (Wang et al. 2003) are the most common voltammetric labels. The AuNPs have the advantages of easy synthesis, good stability, high catalytic activity and good biocompatibility, but they cannot allow for multiple detection in a single assay (Chumbimuni-Torres et al. 2006; Zhu et al. 2013). The QDs may offer the attractive alternative to metal nanoparticles as the voltammetric labels (Dong et al. 2010; Kokkinos et al. 2018; Xiang et al. 2011). The QDs are semiconducting nanoparticles (e.g., PbX, CdX, ZnX (X = S, Se, Te)) with 100-100,000 atoms per particle (Esteve-Turrillas and Abad-Fuentes 2013; Hu et al. 2017; Zhou et al. 2015), and they can be applied for multiplex detection of DNAs and proteins in a single assay using different kinds of QDs (Hansen et al. 2006; Li et al. 2010; Zheng et al. 2014). However, ultrasensitive stripping voltammetric detection of telomerase activity has not been explored so far. In this research, we develop a simple QD-based electrochemical biosensor for stripping voltammetric detection of telomerase activity at the single-cell level. The presence of telomerase enables the addition of the telomere repeats of $(TTAGGG)_n$ to the 3' end of the primer, accompanied by the incorporation of abundant biotins in the extension product. The subsequent hybridization of extension product with the capture DNA and the addition of streptavidin-coated QDs induce the assembly

of large amounts of QDs onto the electrode. After the acidic dissolution of QDs, the released Cd (II) can be simply quantified by ASV. This biosensor can detect telomerase activity at the single-cell level without the involvement of any thermal cycling and extra enzymes for signal amplification.

## 2 Materials and methods

### 2.1 Materials

The primer (5'- AAT CCG TCG AGC AGA GTT-3') and the capture DNA (5'-AAC CCT AAC CCT AAC TCT GCA AAA AAA AAA-$(CH_2)_6$-SH-3') were synthesized by Sangon Biotech (Shanghai, China). The streptavidin-coated CdSe/ZnS QDs with the maximum emission of 605 nm (Qdot 605 ITK) and the mixture nucleotides (dNTPs, including biotin-dATPs, dTTPs and dGTPs) were purchased from Invitrogen Corporation (CA, USA). The TRAPeze 1× CHAPS lysis buffer was purchased from Millipore (Bedford, MA, USA). Telomerase inhibitor MST-312 (N,N'-1,3-Phenylenebis-[2,3-dihydroxy-benzamide]) was purchased from Calbiochem (Gibbstown, NJ, USA). All other chemical agents were obtained from Sigma-Aldrich (St. Louis, MO, USA). Ultrapure water obtained from a Millipore filtration system was used in all experiments. Human cervical cancer cells (HeLa cells), human embryonic kidney cell line (HEK293T cells), and normal human lung cell line (MRC-5 cells) were purchased from Cell Bank of Chinese Academy of Sciences (Shanghai, China).

### 2.2 Cell Culture and Preparation of Telomerase Extracts

Different cell lines including HeLa cells, HEK293T cells and MRC-5 cells were cultured in Dulbecco's modified Eagle's medium (DMEM) with 10% fetal bovine serum and 50 U $mL^{-1}$ penicillin plus 50 μg $mL^{-1}$ streptomycin in a humidified chamber containing 5% $CO_2$ at 37 °C. For telomerase extraction, cells in the exponential phase of growth were collected and resuspended in 200 μL of ice-cold 1× CHAPS lysis buffer (0.5% CHAPS, 1 mM $MgCl_2$, 1 mM EGTA, 0.1 mM PMSF, 5 mM mercaptoethanol, 10% glycerol, 10 mM Tris-HCl, pH 7.5), and incubated on ice for 30 min, followed by centrifugation at 12000 g for 20 min at 4 °C. After centrifugation, the supernatant was carefully transferred into a fresh tube and stored at -80 °C until use.

### 2.3 Fabrication of the biosensor

Prior to the modification, the Au electrode was polished to a mirror-like surface with 1.0, 0.3 and 0.05 μm α-$Al_2O_3$ slurry, respectively, followed by successive sonication with ethanol and ultrapure water for 3 min to

remove the residual alumina powder. The electrode was immersed into fresh piranha solution (3:1 v/v mixture of concentrated $H_2SO_4$ and 30% $H_2O_2$) for 10 min, followed by a thorough rinse with ultrapure water and drying by nitrogen. Then the electrode was electrochemically cleaned in 0.5 M $H_2SO_4$ solution by potential scanning between -0.2 and +1.6 V at a scan rate of 100 mV $s^{-1}$ until a stable reproducible cyclic voltammogram was obtained.

After washing with ultrapure water and drying in a nitrogen stream, the electrode was incubated with 7 μL of solution containing 0.5 μM capture DNA, 25 μM TCEP (TCEP was used to reduce the disulfide bonded oligonucleotides), and 1× TE buffer (pH 8.2) at room temperature for 12 h to make capture DNA immobilize onto the gold electrode surface via the gold-sulfur chemistry (Liang et al. 2013; Liang et al. 2016). Based on previous research (Liang et al. 2016), the thiolated DNA density increases with the immobilization time and reach a plateau at 6 h, with no significant reduction being observed even after a long incubation time of 12 h. For the convenience of experiments, we used the immobilization time of 12 h (i.e., overnight) in the research. The electrode was then thoroughly rinsed with 1× TE buffer (pH 8.2) and dried under a stream of nitrogen gas. Subsequently, 7 μL of 1% BSA was dropped on the electrode for 25 min to block the unmodified sites. At last, the electrode was thoroughly rinsed and stored at 4 °C prior to use.

**2.4 Telomerase extension reaction**

The 7 μL of telomerase reaction solution containing 23.8 nM primer, 13 μM biotin-dATP, 1 mM dGTP, 1 mM dTTP, 1× PCR buffer (10 mM Tris-HCl, pH 8.3, 50 mM KCl, 1 mM $MgCl_2$), DEPC-treated water and the telomerase extracts (containing RNase inhibitors) was dropped on the gold electrode and incubated at 37 ºC for 80 min. Then the electrode was thoroughly rinsed with the washing buffer. At last, 7 μL of QDs (2 nM) was added to the electrode and incubated at room temperature for 15 min, followed by washing the electrode three times using QD incubation buffer (100 mM Tris-HCl, 3 mM $MgCl_2$, 10 mM $(NH_4)_2SO_4$, pH 8.0).

**2.5 SWV detection of the captured QDs**

After the above reaction, the release of $Cd^{2+}$ from the captured QDs was achieved by dissolving in 100 μL of $HNO_3$ (0.1 M) for 2 h. The resulting solution was then transferred into 9.9 mL of HAc-NaAc buffer (0.1 M, pH 5.0), and the anodic stripping voltammetric measurement was conducted with a mercury film modified glassy carbon working electrode. The anodic stripping measurement was carried out by electrodepositing cadmium at -1.1 V for 200 s and then stripping the potential from -0.9 to -0.2 V with a potential step of 4 mV. The

amplitude and frequency of the square wave were specified as 25 mV and 15 Hz, respectively.

### 2.6 Instruments and electrochemical measurement

All electrochemical measurements were carried out on a CHI 660e electrochemical workstation (CH Instruments Inc., USA) at room temperature with a conventional three-electrode system composed of a platinum wire, a saturated calomel and the gold electrode ($d$ = 2 mm) as counter, reference and working electrodes, respectively. Cyclic voltammetry (CV) measurements were carried out in scanning potential from -0.2 V to 0.6 V with 5 mM $[Fe(CN)_6]^{3-/4-}$ (containing 0.1 M KCl) as the electrolyte. Electrochemical impedance spectroscopic (EIS) measurements were performed in 5 mM $[Fe(CN)_6]^{3-/4-}$ redox couple solution (1:1 molar ratio of $K_3Fe(CN)_6/K_4Fe(CN)_6$) containing 0.1 M KCl over a frequency range from 10 kHz to 0.1 Hz using an alternative voltage with an amplitude of 10 mV, superimposed on a dc potential of 0.20 V (vs SCE). The chronocoulometry measurements were carried out over a range from + 0.2 to -0.5 V at a pulse period of 250 ms in 10 mM Tris-HCl buffer containing 50 μM $Ru(NH_3)_6^{3+}$ (pH 7.4) (Steel et al. 1998). The test buffer solution was bubbled for 15 min with high purity nitrogen prior to the chronocoulometry measurement.

## 3 Results and discussion

### 3.1 Principle of the electrochemical biosensor

The principle of QD-based electrochemical biosensor for stripping voltammetric detection of telomerase activity is shown in Scheme 1. This assay involves four steps: (1) preparation of the gold electrode-based sensor, (2) telomerase-induced primer extension reaction, (3) assembly of QDs, and (4) ASV detection of the release $Cd^{2+}$. The capture DNA modified with a thiol group at the 3' end was attached onto the gold electrode surface via a gold-sulfur bond, and then the electrode surface was blocked with BSA to reduce the nonspecific adsorption of DNAs. The reaction solution containing primer, biotin-dATP, dTTP, dGTP and telomerase extract was dropped onto the electrode and incubated at 37 °C for a certain period of time. The telomerase induces the addition of hexamer repeats $(TTAGGG)_n$ to the 3'-terminal of the primer, leading to the incorporation of a large number of biotin-dATP into the extension product. The subsequent hybridization of extension product with the capture DNA and the addition of streptavidin-coated QDs induce the assembly of large amounts of QDs onto the electrode via specific biotin-streptavidin binding. Due to the availability of

multiple biotins in the extension product, a number of QDs can be assembled on the electrode surface, significantly improving the label efficiency. Moreover, the dissolution of the anchored QDs in nitric acid solution may release large amounts of Cd (II), generating a strong Cd(II) elution peak at -0.74V in the square wave voltammetry measurement. Consequently, the telomerase activity can be detected by the measurement of an electrical current. While in the absence of telomerase, neither telomerase-induced primer extension reaction nor the assembly of QDs on the electrode surface can occur. As a result, no Cd(II) releases upon acid dissolution and no electrical current is detected.

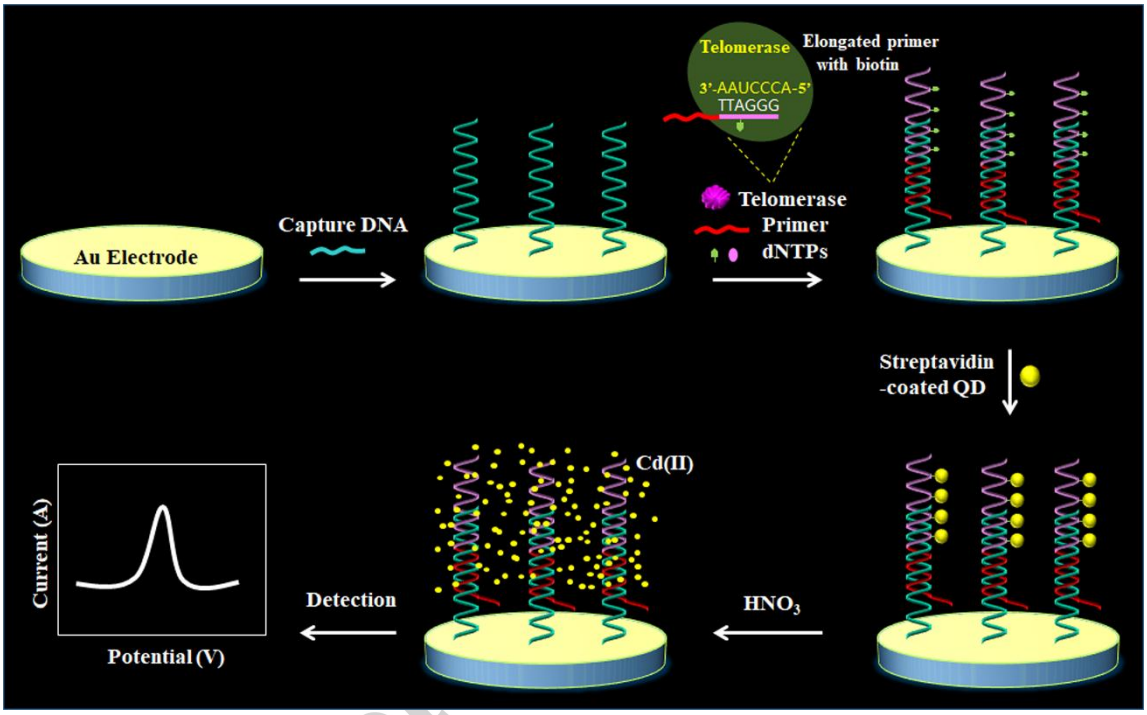


**Scheme 1.** Schematic illustration of QD-based electrochemical biosensor for stripping voltammetric detection of telomerase activity.

### 3.2 Characterization of electrochemical biosensor

To verify the interface property of the modified electrode, cyclic voltammograms (CV) and electrochemical impedance spectra (EIS) were performed for each step of the fabrication process. A pair of well-defined redox peaks is observed on the bare Au electrode with peak potential separation ($\Delta E_p$) of 98 mV, which can be contribute to the good conductivity of the bare gold electrode (Fig. 1A, curve a). These peaks are accredited to the redox behavior of $[Fe(CN)_6]^{3-/4-}$ at electrode surfaces. However, after the immobilization of capture DNA on the Au electrode, the value of $\Delta E_p$ increases to 137 mV (Fig. 1A, curve b). This can be easily explained by

the limited diffusion of the redox species toward the electrode surface of the negative charged phosphate backbone of capture DNA. After the capture DNA/Au electrode is incubated with BSA, the current undergoes a further decrease (Fig. 1A, curve c), which is mainly caused by the blocking effect of BSA. When the extension product is hybridized with capture DNA immobilized on the Au electrode, there is a further decrease of redox current and a further enlargement of peak separation (Fig. 1A, curve d). This can be well explained by the fact that the introduction of extension product induces the increase of the negative charge of the phosphate backbone of DNA and consequently the increased repellence of redox species on the electrode surface. When the streptavidin-coated QDs are assembled onto the electrode surface through the biotin-streptavidin interaction, the peak current increases and the $\Delta E_p$ decreases (Fig. 1A, curve e).

The electrode fabrication process was also monitored by EIS, and the Nyquist plots of the impedance spectra was used to characterize the fabrication procedures of the electrode with $[Fe(CN)_6]^{3-/4-}$ as an electroactive species (Fig. 1B). The bare Au electrode displays a small semicircle diameter and a long tail, indicating the diffusion of $[Fe(CN)_6]^{3-/4-}$ (Fig. 1B, curve a). With the immobilization of capture DNA onto the electrode via the Au-S bond, the value of electron-transfer resistance ($R_{et}$) increases significantly (Fig. 1B, curve b). This can be attributed to the strong electrostatic repulsion between the negatively charged redox indicator ferricyanide and the phosphoric acid groups of the DNA backbone. After the electrode is blocked by BSA, the value of $R_{et}$ further increases (Fig. 1B, curve c), which results from the blocking of interfacial electron transfer by BSA. The value of $R_{et}$ increases remarkably after the hybridization of extension product with the capture DNA (Fig. 1B, curve d). This can be ascribed to the repulsion of the negatively charged redox indicator ferricyanide by the hybridized extension product. Interestingly, the binding of QDs to the extension product induces the decrease of $R_{et}$ (Fig. 1B, curve e), consistent with the previous research (Huang et al. 2010). These results indicate that the stepwise electrode fabrication process is successful.

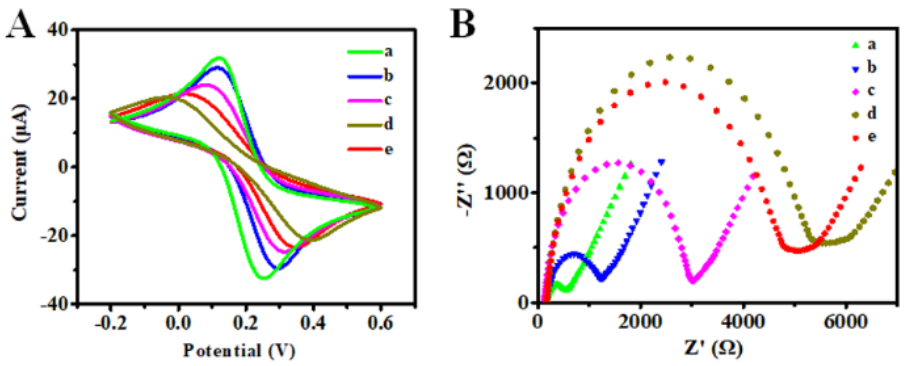


**Fig. 1.** (A) Cyclic voltammograms and (B) electrochemical impedance spectra (Nyquist plots) of different modified electrodes in 0.1 M KCl solution containing 5 mM $[Fe(CN)_6]^{3-/4-}$: (a) bare Au electrode, (b) capture DNA/Au electrode, (c) BSA/capture DNA/Au electrode, (d) BSA/extension product-capture DNA hybrids/Au electrode, and (e) the assembly of QDs onto BSA/extension product-capture DNA hybrids/Au electrode.

### 3.3 Optimization of experimental conditions

The detection sensitivity and selectivity of this assay is influenced by the experimental conditions including the time of BSA blocking the Au electrode, the concentrations of capture DNA and biotin-dATP, the extension time of telomerase, and the deposition time of $Cd^{2+}$. In this assay, the blocking agent BSA was added to eliminate the nonspecific binding of QDs onto the electrode surface (Kokkinos et al. 2018), and the duration of the blocking should be optimized. As shown in Fig. 2A, the peak current in the absence of telomerase extract ($I_0$) decreases with the blocking time, and 25-min blocking may efficiently minimize the signal resulting from the nonspecific binding. Thus, the blocking time of 25 min is used in the subsequent research.

The concentration of capture DNA is crucial to the assembly of QDs onto the electrode surface and should be optimized carefully. As shown in Fig. 2B, the value of $I - I_0$ enhances with the increasing concentration of capture DNA from 100 to 500 nM ($I$ and $I_0$ represent the peak current in the presence and absence of telomerase extract, respectively), followed by the decrease beyond the concentration of 500 nM. This may be explained by following factors: the more DNA being modified on the electrode the more extension products being hybridized, the more QDs being assembled on the electrode surface and consequently the higher peak current. However, the high-concentration capture DNA may cause steric

hindrance to prevent the assembly of QDs onto the electrode surface, leading to the decrease of peak current. Thus, 500 nM capture DNA is used in the subsequent research. We further optimized the concentration of biotin-dATP. As shown in Fig. 2C, the peak current improves with the increasing concentration of biotin-dATP from 5 to 13 μM, and levels off at the concentration of 13 μM. Thus, 13 μM biotin-dATP is used in the subsequent research.

We optimized the telomerase extension time as well. As shown in Fig. 2D, the peak current enhances with the telomerase extension time, and reaches the maximum value at 80 min. Thus, the extension time of 80 min is used in the subsequent research. The electrolytic deposition time of Cd(II) significantly influences the signal of stripping voltammetry and should be optimized. As shown in Fig. 2E, the peak current increases with the deposition time, and reaches the maximum value at 200 s. Thus, the deposition time of 200s is used in the subsequent research.

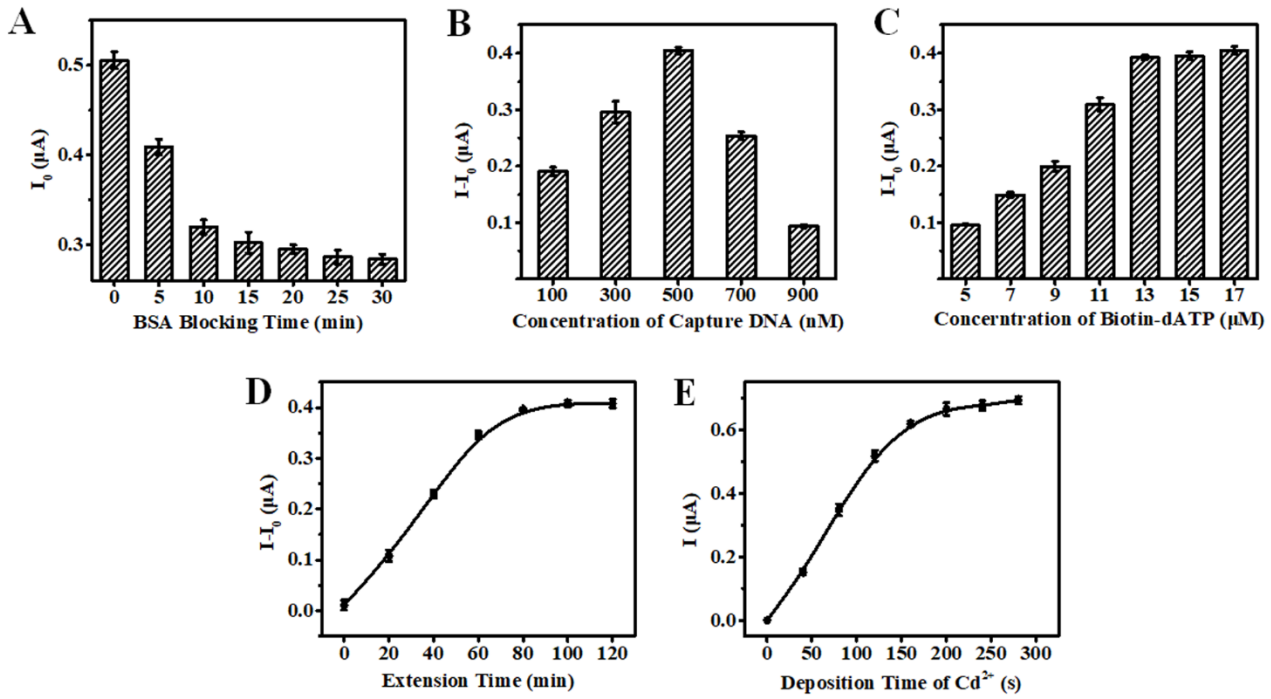


**Fig. 2**. (A) Variance of the peak current ($I_0$) with the BSA blocking time. (B) Variance of the $I$ — $I_0$ value with the concentration of capture DNA. (C) Variance of the $I$-$I_0$ value with the concentration of biotin-dATP. (D) Variance of the $I$ — $I_0$ value with the telomerase extension time. (E) Variance of the peak current ($I$) with the deposition time of Cd (II). $I$ and $I_0$ represent the peak current in the presence and absence of telomerase extracts. The HeLa cell extracts are equivalent to $10^6$ cells. The error bars represent the standard deviations of

three experiments.

### 3.4 Quantitation of DNA density on the electrode surface

The density of the electrode surface-confined capture DNA can be estimated electrochemically via chronocoulometry. The charge Q as a function of time t in a chronocoulometric experiment is given by the integrated Cottrell expression (Steel et al. 1998) with $[Ru(NH_3)_6]^{3+}$ as the redox mediator.

$$Q = \frac{2nFAD_0^{1/2}C_0^*}{\pi^{1/2}} t^{1/2} + Q_{dl} + nFA\Gamma_0 \qquad (1)$$

Where $Q_{dl}$ is the capacitive charge, and $nFA\Gamma_0$ represents the charge produced by the adsorbed $[Ru(NH_3)_6]^{3+}$. The amount of $[Ru(NH_3)_6]^{3+}$ adsorbed onto the phosphate backbone of the immobilized DNA ($\Gamma_0$), which can be determined from the difference in intercepts ($\Delta_{int}$) at $t$ = 0 in the presence and absence of $[Ru(NH_3)_6]^{3+}$ (Zhang et al. 2006), is quantitative to the amount of the immobilized DNA ($\Gamma_{DNA}$) by dividing the number of bases in the single immobilized DNA strand:

$$\Gamma_{DNA} = \Gamma_0(z/m)(N_A) \qquad (2)$$

where $\Gamma_{DNA}$ is the surface density of the electrode surface-attached DNA, $m$ is the number of bases in DNA, $z$ is the charge of redox molecule (z is 3 for $[Ru(NH_3)_6]^{3+}$), and $N_A$ is Avogadro's number. Based on the chronocoulometric responses of $[Ru(NH_3)_6]^{3+}$ (Fig. 3), the surface density of capture DNA on the gold electrode surface is estimated to be 3.2 (± 0.1) × $10^{12}$ molecules $cm^{-2}$, consistent with the previous research (3.0 ~ 3.94 × $10^{12}$ molecules $cm^{-2}$) (Cui et al. 2018; Liang et al. 2016).

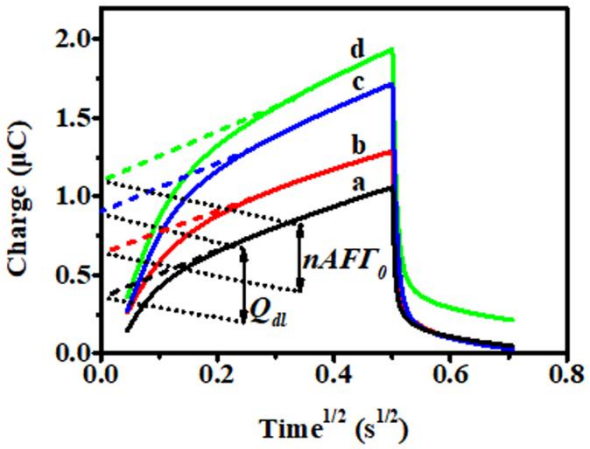


**Fig. 3.** Chronocoulometric response of MCH (a, c) and DNA/MCH (b, d) modified electrodes in the absence (a, b) and presence of 50 μM $[Ru(NH_3)_6]^{3+}$ (c, d). Redox charges of $[Ru(NH_3)_6]^{3+}$ bound to DNA are obtained

from chronocoulometric intercepts at $t = 0$.

### 3.5 Detection Sensitivity

To investigate the detection sensitivity, we measured the peak currents in response to the different number of HeLa cells using square wave anodic stripping voltammetry (SWASV). As shown in Fig. 4A, a well-defined anodic stripping peak at -0.74 V is observed as a result of the release of Cd (II) from the QDs. The value of -0.74 V is consistent with the reported stripping peaks of Cd (II) (-0.68 V ~ -0.78 V) (Wang et al. 2003; Zheng et al. 2014). The current signal enhances with the increase of HeLa cell number from 0 to $10^5$ cells and reaches a plateau at $10^6$ cells (Fig. 4A), and the telomerase activity can be quantified by measuring the SWASV peak current at -0.74 V (Fig. 4B). Notably, the peak current exhibits a good correlation with the logarithm of the HeLa cell number in the range from 1 to $10^5$ cells (inset of Fig. 4B). The regression equation is $I - I_0 = 0.0682 \log_{10} N + 0.0525$ with a correlation coefficient of 0.994, where $I$ and $I_0$ are the peak current in the presence and absence of telomerase extracts, respectively, and $N$ is the number of HeLa cell. The limit of detection (LOD) is calculated to be 0.37 cells based on $3\sigma/K$, where $\sigma$ is the standard deviation of the control group without telomerase extracts and $K$ is the slope of the linear regression curve, suggesting the sensitivity of the proposed method can reach single-cell level. We further measured the peak currents signals in response to the different number of HEK293T cells. As shown in Fig. 4C, the current signal improves with the increasing number of HEK293T cell. The peak current at -0.74 V exhibits a good correlation with the logarithm of the logarithm of the HEK293T cell number in the range from 10 to $10^5$ cells (inset of Fig. 4D). The regression equation is $I - I_0 = 0.0709 \log_{10} N + 0.0137$ with a correlation coefficient of 0.990, where $I$ and $I_0$ are the peak current in the presence and absence of telomerase extracts, respectively, and $N$ is the number of HEK293T cell. The LOD is estimated to be 1.2 cell based on $3\sigma/K$. Notably, the sensitivity of the proposed method is comparable to / even much higher than those of enzyme-based methods such as exponential isothermal amplification-based real-time fluorescence method (1 HeLa cell) (Tian and Weizmann 2013), and primer-generation rolling circle amplification-based fluorescent assay (3 HeLa cells) (Ma et al. 2018), and enzyme-free methods such as AuNP-involved dual signal amplification-based electrochemical assay (2 HeLa cells) (Wang et al. 2015b), and AuNP aggregation-based optical assay (27 HEK293T cells/μL) (Sharon et al. 2014). The high sensitivity of the proposed method can be attributed to following three factors:

(1) the telomerase-induced sequential addition of biotin molecules to the ends of primer, (2) the assembly of abundant QDs onto the electrode surface via specific biotin-streptavidin interaction, and (3) the high signal amplification efficiency induced by the release of numerous Cd (II) ions from QDs, which can accurately quantified by stripping voltammetry (Xiang et al. 2011).

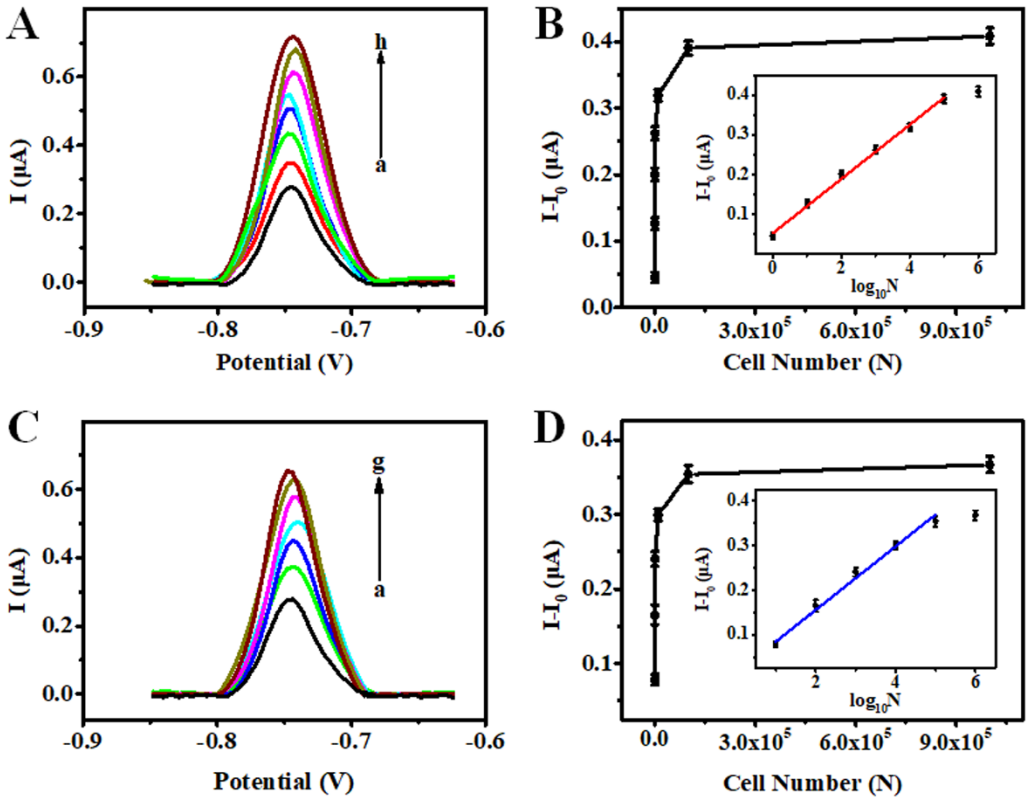


**Fig. 4.** (A) SWASV current spectra in response to telomerase extracts from different number of HeLa cell: 0, 1, 10, $10^2$, $10^3$, $10^4$, $10^5$, $10^6$ cells (from a to h). (B) Dependence of SWASV peak current at -0.74 V upon HeLa cell number. Inset shows the linear relationship between the $I$ — $I_0$ value and the logarithm of HeLa cell number in the range from 1 to $10^5$ cells. (C) SWASV current spectra in response to telomerase extracts from different number of HEK293T cell: 0, 10, $10^2$, $10^3$, $10^4$, $10^5$, $10^6$ cells (from a to g). (D) Dependence of SWASV peak current at -0.74 V on HEK293T cell number. Inset shows the linear relationship between the $I$ — $I_0$ value and the logarithm of HEK293T cell number in the range from 10 to $10^5$ cells. The error bars represent the standard deviations of four experiments.

### 3.6 Detection specificity

To investigate the detection specificity, we measured the peak currents in response to MRC-5 cells, HeLa

cells and HEK293T cells, respectively. MRC-5 cells are somatic cells without overexpression of telomerase (Tian and Weizmann 2013), while HeLa cells and HEK293T cells are cancer cells. As shown in Fig. 5A, MRC-5 cells do not induce significant change in peak current (Fig. 5A, column a) compared with the heat-treated HeLa cells (Fig. 5A, column b) and heat-treated HEK293T cells (Fig. 5A, column c). This can be explained by the factor that heat-treatment can destroy reverse transcriptase protein and telomerase RNA and consequently deactivates telomerase. In contrast, both HEK293T cells (Fig. 5A, columns d) and HeLa cells (Fig. 5A, columns e) display high $I - I_0$ value, indicating the high activity of telomerase in cancer cells (Kim et al. 1994). Notably, the measured $I - I_0$ value of HEK293T cells (Fig. 5A, columns d) is similar to that of HeLa cells (Fig. 5A, columns e), suggesting the same expression level of telomerase for HEK293T cells and HeLa cells, consistent with the reported telomerase monomers per cell for HeLa cells (240 ± 20) and HEK293T cells (240 ± 90) obtained by direct enzyme assay (Xi and Cech 2014). These results clearly demonstrate that the proposed method can be used to monitor the cellular telomerase activity and discriminate cancer cells from normal cells.

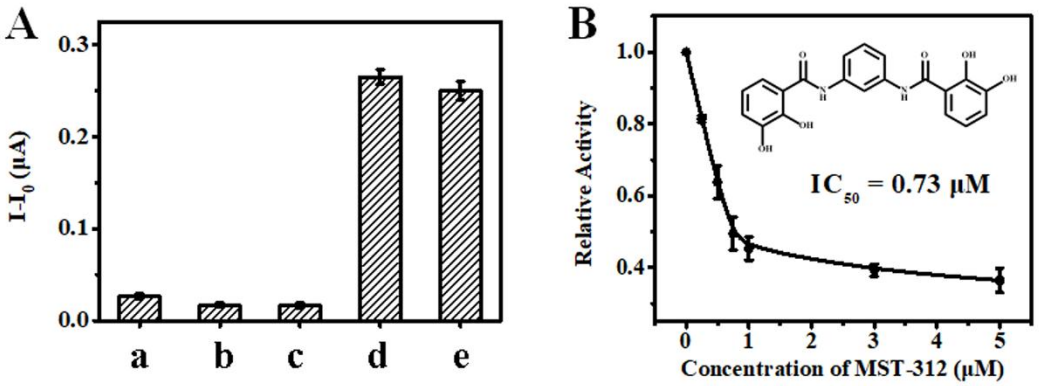


**Fig. 5.** (A) Measurement of telomerase activity from different cell line extracts: MRC-5 cells (a), heat-treated HeLa cells (b), heat-treated HEK293T cells (c), HeLa cells (d), and HEK293T cells (e). All the cell extracts are equivalent to1000 cells. (B) Inhibition effects of MST-312 on telomerase activity of HeLa cells. Inset shows the chemical structure of MST-312. The error bars represent the standard deviations of three experiments.

### 3.7 Inhibition assay

High telomerase activity are observed in cancer cells and the screening of telomerase inhibitors can be used

for anticancer drug discovery (Arndt and MacKenzie 2016; Sekaran et al. 2014). We further investigated the feasibility of the proposed method for inhibition assay with the tea catechin derivative MST-312 (N,N'-1,3-Phenylenebis-[2,3-dihydroxy-benzamide]) as the inhibitor (Gurung et al. 2014; Seimiya et al. 2002). We measured the peak currents in response to different-concentration MST-312 after treatment with HeLa cell extracts. The relative activity (*RA*) is determined as $RA = (I_i - I_0) / (I - I_0)$, where $I_0$ is the peak current in the absence of telomerase, $I$ is the peak current in the presence of telomerase without the inhibitor treatment, and $I_i$ is the current in the presence of both telomerase and the inhibitor, respectively. As illustrated in Fig. 5B, the relative activity of telomerase decreases with the increasing concentration of MST-312. The $IC_{50}$ value (i.e., the concentration for the inhibition of telomerase activity by 50%) is determined to be 0.73 μM, consistent with that obtained by PCR-based TRAP assay (0.67 μM) (Seimiya et al. 2002). This result indicates that the proposed method can be used for the screening of telomerase inhibitors.

**Conclusions**

In summary, we have developed a simple QD-based electrochemical biosensor for stripping voltammetric detection of telomerase activity at the single-cell level. Taking advantage of (1) the telomerase-induced sequential addition of biotin molecules to the ends of primer, (2) the assembly of abundant QDs onto the electrode surface via specific biotin-streptavidin interaction, and (3) the high signal amplification efficiency induced by the stripping voltammetry detection of the released Cd (II) ions from QDs (Xiang et al. 2011), this biosensor can detect telomerase at the single-cell level and exhibits an extremely large dynamic range from 1 to $10^5$ cells, which is superior to the reported optical method for telomerase assay (Ma et al. 2018; Sharon et al. 2014). In comparison with the PCR-based TRAP and isothermal nucleic acid amplification-based assays (Kim et al. 1994; Tian and Weizmann 2013), this biosensor does not involve any thermal cycling, complicated template and probe design, and the use of special enzymes. Importantly, this biosensor has significant advantages of high sensitivity, simplicity, rapidity, PCR-free and enzyme-free, and it can be used for the monitoring of cellular telomerase activity and the discrimination of cancer cells from normal cells as well as the screening of telomerase inhibitors, holding great potential for further applications in clinical diagnosis and anticancer drug discovery.

**ACKNOWLEDGMENT**

This work was supported by the National Natural Science Foundation of China (Grant Nos. 21325523, 21527811, 21735003 and 21575152), the Project of Shandong Province Higher Educational Science and Technology Program (Grant No. J16LC08), and the Award for Team Leader Program of Taishan Scholars of Shandong Province, China.

**Notes**

The authors declare no competing financial interest.

**References**

Alizadeh-Ghodsi, M., Zavari-Nematabad, A., Hamishehkar, H., Akbarzadeh, A., Mahmoudi-Badiki, T., Zarghami, F., Moghaddam, M.P., Alipour, E., Zarghami, N., 2016. Biosens. Bioelectron. 80, 426-432.

Arndt, G.M., MacKenzie, K.L., 2016. Nat. Rev. Cancer 16, 508-524.

Blackburn, E.H., 2001. Cell 106, 661-673.

Chumbimuni-Torres, K.Y., Dai, Z., Rubinova, N., Xiang, Y., Pretsch, E., Wang, J., Bakker, E., 2006. J. Am. Chem. Soc. 128, 13676-13677.

Cohen, S.B., Graham, M.E., Lovrecz, G.O., Bache, N., Robinson, P.J., Reddel, R.R., 2007. Science 315, 1850-1853.

Collins, K., Mitchell, J.R., 2002. Oncogene 21, 564-579.

Cui, L., Li, Y., Lu, M., Tang, B., Zhang, C.Y., 2018. Biosens. Bioelectron. 99, 1-7.

De Cian, A., Cristofari, G., Reichenbach, P., De Lemos, E., Monchaud, D., Teulade-Fichou, M.-P., Shin-Ya, K., Lacroix, L., Lingner, J., Mergny, J.-L., 2007. Proc. Natl. Acad. Sci. U. S. A. 104, 17347-17352.

Dong, H., Yan, F., Ji, H., Wong, D.K.Y., Ju, H., 2010. Adv. Funct. Mater. 20, 1173-1179.

Esteve-Turrillas, F.A., Abad-Fuentes, A., 2013. Biosens. Bioelectron. 41, 12-29.

Gao, W., Nyein, H.Y.Y., Shahpar, Z., Fahad, H.M., Chen, K., Emaminejad, S., Gao, Y., Tai, L.-C., Ota, H., Wu, E., Bullock, J., Zeng, Y., Lien, D.-H., Javey, A., 2016. ACS Sens. 1, 866-874.

Gurung, R.L., Lim, S.N., Low, G.K.M., Hande, M.P., 2014. J. Nutrigenet. Nutrigenomics 7, 283-298.

Hansen, J.A., Wang, J., Kawde, A.-N., Xiang, Y., Gothelf, K.V., Collins, G., 2006. J. Am. Chem. Soc. 128, 2228-2229.

Harley, C.B., 2008. Nat. Rev. Cancer 8, 167-179.

Hu, J., Wang, Z.-y., Li, C.-c., Zhang, C.-y., 2017. Chem. Commun. 53, 13284-13295.

Huang, H., Li, J., Tan, Y., Zhou, J., Zhu, J.-J., 2010. Analyst 135, 1773-1778.

Kim, N.W., Piatyszek, M.A., Prowse, K.R., Harley, C.B., West, M.D., Ho, P.L., Coviello, G.M., Wright, W.E., Weinrich, S.L., Shay, J.W., 1994. Science 266, 2011-2015.

Kokkinos, C.T., Giokas, D.L., Economou, A.S., Petrou, P.S., Kakabakos, S.E., 2018. Anal. Chem. 90, 1092-1097.

Li, X., Liu, J., Zhang, S., 2010. Chem. Commun. 46, 595-597.

Liang, G., Liu, X., Li, X., 2013. Biosens. Bioelectron. 45, 46-51.

Liang, G., Man, Y., Jin, X., Pan, L., Liu, X., 2016. Anal. Chim. Acta 936, 222-228.

Ma, F., Wei, S.-h., Leng, J., Tang, B., Zhang, C.-y., 2018. Chem. Commun. 54, 2483-2486.

Martinez, P., Blasco, M.A., 2011. Nat. Rev. Cancer 11, 161-176.

Qian, R., Ding, L., Ju, H., 2013. J. Am. Chem. Soc. 135, 13282-13285.

Seimiya, H., Oh-hara, T., Suzuki, T., Naasani, I., Shimazaki, T., Tsuchiya, K., Tsuruo, T., 2002. Mol. Cancer Ther. 1, 657-665.

Sekaran, V., Soares, J., Jarstfer, M.B., 2014. J. Med. Chem. 57, 521-538.

Sharon, E., Golub, E., Niazov-Elkan, A., Balogh, D., Willner, I., 2014. Anal. Chem. 86, 3153-3158.

Shay, J.W., Wright, W.E., 2011. Semin. Cancer Biol. 21, 349-353.

Steel, A.B., Herne, T.M., Tarlov, M.J., 1998. Anal. Chem. 70, 4670-4677.

Stone, M.D., Mihalusova, M., O'Connor, C.M., Prathapam, R., Collins, K., Zhuang, X., 2007. Nature 446, 458-461.

Su, D., Huang, X., Dong, C., Ren, J., 2018. Anal. Chem. 90, 1006-1013.

Tian, L., Weizmann, Y., 2013. J. Am. Chem. Soc. 135, 1661-1664.

Wang, F., Li, W., Wang, J., Ren, J., Qu, X., 2015a. Chem. Commun. 51, 11630-11633.

Wang, H.-B., Wu, S., Chu, X., Yu, R.-Q., 2012a. Chem. Commun. 48, 5916-5918.

Wang, J., Liu, G., Merkoci, A., 2003. J. Am. Chem. Soc. 125, 3214-3215.

Wang, L.-j., Ma, F., Tang, B., Zhang, C.-y., 2017a. Chem. Sci. 8, 2495-2502.

Wang, L., Leng, C., Tang, S., Lei, J., Ju, H., 2012b. Biosens. Bioelectron. 38, 421-424.

Wang, W.-J., Li, J.-J., Rui, K., Gai, P.-P., Zhang, J.-R., Zhu, J.-J., 2015b. Anal. Chem. 87, 3019-3026.

Wang, Y., Yang, L., Li, B., Yang, C.J., Jin, Y., 2017b. Anal. Chem. 89, 8311-8318.

Xi, L., Cech, T.R., 2014. Nucleic Acids Res. 42, 8565-8577.

Xiang, Y., Zhang, H., Jiang, B., Chai, Y., Yuan, R., 2011. Anal. Chem. 83, 4302-4306.

Xiao, Y., Dane, K.Y., Uzawa, T., Csordas, A., Qian, J., Soh, H.T., Daugherty, P.S., Lagally, E.T., Heeger, A.J., Plaxco, K.W., 2010. J. Am. Chem. Soc. 132, 15299-15307.

Zhang, H.-R., Wang, Y.-Z., Wu, M.-S., Feng, Q.-M., Shi, H.-W., Chen, H.-Y., Xu, J.-J., 2014. Chem. Commun. 50, 12575-12577.

Zhang, J., Song, S., Zhang, L., Wang, L., Wu, H., Pan, D., Fan, C., 2006. J. Am. Chem. Soc. 128, 8575-8580.

Zhang, Q., Li, L., Qiao, Z., Lei, C., Fu, Y., Xie, Q., Yao, S., Li, Y., Ying, Y., 2017. Anal. Chem. 89, 12145-12151.

Zheng, L., Li, X., Liu, P., Wu, G., Lu, X., Liu, X., 2014. Biosens. Bioelectron. 52, 354-359.

Zhou, J., Yang, Y., Zhang, C.-y., 2015. Chem. Rev. 115, 11669-11717.

Zhu, Y., Chandra, P., Shim, Y.-B., 2013. Anal. Chem. 85, 1058-1064.

## Highlights

- A simple quantum dot (QD)-based electrochemical biosensor is developed for stripping voltammetric detection of telomerase activity.
- This biosensor can detect telomerase activity at the single-cell level.
- This biosensor can be used for the discrimination of cancer cells from normal cells and the screening of telomerase inhibitors.
- This biosensor has significant advantages of high sensitivity, simplicity, rapidity, PCR-free and enzyme-free.